Highway Traffic State Estimation With Mixed Connected and Conventional Vehicles

Nikolaos Bekiaris-Liberis, Claudio Roncoli, and Markos Papageorgiou, *Fellow, IEEE*

Abstract—We present a macroscopic model-based approach for the estimation of the total density and flow of vehicles, for the case of "mixed" traffic, i.e., traffic comprising both ordinary and connected vehicles, utilizing only average speed measurements reported by connected vehicles and a minimum number (sufficient to guarantee observability) of spot-sensor-based total flow measurements. The approach is based on the realistic and validated assumption that the average speed of conventional vehicles is roughly equal to the average speed of connected vehicles, and consequently, it can be obtained at the (local or central) traffic monitoring and control unit from connected vehicles' reports. Thus, complete traffic state estimation (for arbitrarily selected segments in the network) may be achieved by estimating the total density of vehicles. Recasting the dynamics of the total density of vehicles, which are described by the well-known conservation law equation, as a linear parameter-varying system, we employ a Kalman filter for the estimation of the total density. We demonstrate the fact that the developed approach allows for a variety of different measurement configurations. We also present an alternative estimation methodology in which traffic state estimation is achieved by estimating the percentage of connected vehicles with respect to the total number of vehicles. The alternative development relies on the alternative requirement that the density and flow of connected vehicles are known to the traffic monitoring and control unit on the basis of their regularly reported positions. We validate the performance of the developed estimation schemes through simulations using a well-known second-order traffic flow model as ground truth for the traffic state.

Index Terms—Traffic estimation, connected vehicles.

I. INTRODUCTION

A NUMBER of novel Vehicle Automation and Communication Systems (VACS) have already been introduced, and many more are expected to be introduced in the next years. These systems are mainly aimed to improve driving safety and convenience, but are also believed to have great poten-

tial in mitigating traffic congestion, if appropriately exploited for innovative traffic management and control [11]. To attain related traffic flow efficiency improvements on highways, it is of paramount importance to develop novel methodologies for modeling, estimation and control of traffic in presence of VACS. Several papers are providing useful results related to modeling and control of traffic flow in presence of VACS, employing either microscopic or macroscopic approaches, see, for example, [6]–[8], [12], [16], [17], [26], [32]–[36], [38], [41], [43], [44], [48], [51].

The availability of reliable real-time measurements or estimates of the traffic state is a prerequisite for successful highway traffic control. In conventional traffic, the necessary measurements are provided by spot sensors (based on a variety of possible technologies), which are placed at specific highway locations. If the sensor density is sufficiently high (e.g., every 500 m), then the collected measurements are usually sufficient for traffic surveillance and control; else, appropriate estimation schemes need to be employed in order to produce traffic state estimates at the required space resolution (typically 500 m); see, for instance, [1], [15], [19], [22], [24], [25], [46], among many other works addressing highway traffic estimation by use of conventional detector data. However, the implementation and maintenance of road-side detectors entail considerable cost; hence various research works attempt to exploit different, less costly data sources, such as mobile phone, or GPS (Global Positioning System), or even vehicle speed data for travel time or highway state estimation; employing various kinds of traffic [2], [4], [13], [14], [29], [47], [49], [50] or statistic [10], [37] models, or by developing data-fusion techniques [9], [27], [31], [39], [42].

In fact, with the introduction of VACS of various kinds, an increasing number of vehicles become "connected," i.e., enabled to send (and receive) real-time information to a local or central monitoring and control unit (MCU). Thus, connected vehicles may communicate their position, speed and other relevant information, i.e., they can act as mobile sensors. This may allow for a sensible reduction (and, potentially, elimination) of the necessary number of spot sensors, which would lead to according reduction of the purchase, installation, and maintenance cost for traffic monitoring. This paper concerns the development of reliable and robust traffic state estimation methods, which exploit information provided by connected vehicles and reduces the need for spot sensor measurements under all penetration rates of connected vehicles, i.e., for a mixed traffic flow that includes both conventional and connected vehicles.

The authors are with the Department of Production Engineering and Management, Technical University of Crete, 73100 Chania, Greece (e-mail: nikos.bekiaris@gmail.com; croncoli@dssl.tuc.gr; markos@dssl.tuc.gr).

Specifically, we address the problem of estimating the (total) density and flow of vehicles in highway segments of arbitrary length (typically around 500 m) in presence of connected vehicles. The developments rely on the realistic assumption that the average speed of conventional vehicles is roughly equal to the average speed of connected vehicles, and consequently, the average speed of all vehicles on an arbitrary segment of the highway can be readily obtained at the local or central MCU from connected vehicles reports. This assumption, which is indeed validated by use of real data, relies on the fact that, even at very low densities, there is no reason for connected vehicles to feature a systematically different mean speed than conventional vehicles; while at higher densities, the assumption is further reinforced due to increasing difficulty of overtaking. As a consequence of this assumption, complete traffic state estimation (of the total density and flow in arbitrary segments in the highway) may be achieved via estimating the traffic density by utilizing average speed measurements from connected vehicles together with a minimum (necessary to guarantee observability) amount of conventional measurements of traffic volumes, e.g., at all entries and exits of the considered highway stretches. The developed estimation methodology allows a variety of different conventional measurement configurations.

An alternative estimation approach is also developed, in which traffic state estimation is achieved by estimating the percentage of connected vehicles with respect to the total number of vehicles. This alternative estimation approach relies on the additional, yet natural, requirement that the density and flow of connected vehicles may be readily obtained at the local or central MCU on the basis of their regularly reported positions.

The performance of the developed estimation schemes is validated through simulations using the well-known METANET traffic flow model as ground truth for the traffic state, including the case in which the speed of connected vehicles is reported to the MCU with a communication delay.

In more technical terms, the dynamics of the total traffic density, as described by the well-known (discrete-time) conservation law equation, are recast as a linear parameter-varying system with known parameters that depend on the real-time average speed measurements (Section II-A), thus removing the requirement of (empirical, hence uncertain) traffic speed modeling, such as the fundamental diagram. The observability properties of this system are studied (Section II-B) and a Kalman filter is employed for the estimation of the total density of vehicles (Section II-C). The effectiveness of the proposed estimation design is illustrated in simulation with a second-order macroscopic model as ground truth (Section III). The estimation approach is then extended to the case of unmeasured total flows at on-ramps or off-ramps (by incorporating additional mainstream total flow measurements that replace a corresponding number of total flow measurements at on-ramps or off-ramps) and its performance in this case is also illustrated in simulation (Section IV). In the alternative estimation approach a linear parameter-varying model is derived for the dynamics of the percentage of connected vehicles and a Kalman filter is employed for its estimation (Section V).
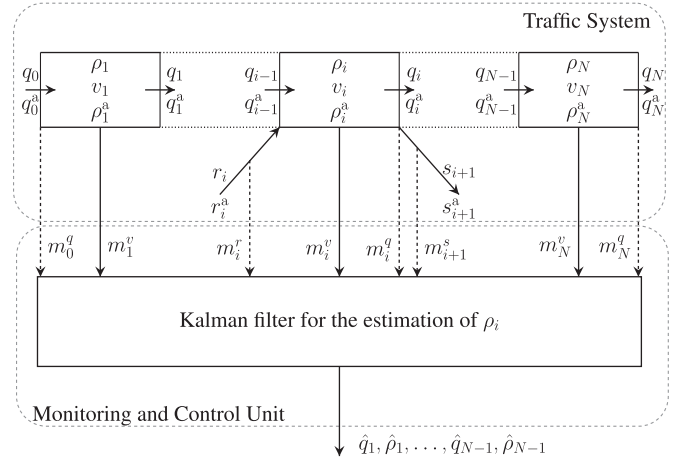

Fig. 1. Traffic system under consideration and the Kalman filter implemented at the MCU. The data used to operate the Kalman filter are either speed measurements coming from connected vehicles (solid lines) or flow measurements coming from fixed sensors (dashed lines). The variable m_i^w denotes the measurement of quantity w at segment i, which might be different than the actual quantity w, due to, for example, the presence of measurement noise. A variable w_i^a represents the value of quantity w of connected vehicles at segment i.

II. TRAFFIC ESTIMATION USING AVERAGE SPEED MEASUREMENTS FROM CONNECTED VEHICLES

A. Dynamics of Traffic Density as a Linear Parameter-Varying System

We consider the following discrete-time equations that describe the dynamics of the total densities ρ_i of vehicles on highway segments (see, e.g., [28]; see also the upper part of Fig. 1)

$$\rho_i(k+1) = \rho_i(k) + \frac{T}{\Delta_i}(q_{i-1}(k) - q_i(k) + r_i(k) - s_i(k)) \tag{1}$$

where $i = 1, \ldots, N$ is the index of the specific segment at the highway, N being the number of segments on the highway; for all traffic variables, we denote by index sub-i its value at the segment i of the highway; q_i is the total flow at segment i; T is the time-discretization step, Δ_i is the length of segment i, and $k = 0, 1, \ldots$ is the discrete time index. The variables r_i and s_i denote the inflow and outflow of vehicles at on-ramps and off-ramps, respectively, at segment i. Using the known relation

$$q_i = \rho_i v_i \tag{2}$$

where v_i is the average speed in segment i, we write (1) as

$$\rho_i(k+1) = \frac{T}{\Delta_i}v_{i-1}(k)\rho_{i-1}(k) + \left(1 - \frac{T}{\Delta_i}v_i(k)\right)\rho_i(k) + \frac{T}{\Delta_i}(r_i(k) - s_i(k)). \tag{3}$$

Assuming that the average speed of conventional vehicles is roughly equal to the average speed of connected vehicles, and hence, it can be reported to the traffic authority from the connected vehicles, one can conclude that $v_i, i = 1, \ldots, N$, are measured. Therefore, defining the state

$$x = (\rho_1, \ldots, \rho_N)^T \tag{4}$$

system (3) can be written in the form of a known linear parameter-varying system of the form

$$x(k+1) = A(v(k)) x(k) + Bu(k) \qquad (5)$$

$$y(k) = Cx(k) \qquad (6)$$

where

$$A(v(k)) = \begin{cases} a_{ij} = \frac{T}{\Delta_i} v_{i-1}(k), & \text{if } i-j=1 \\ & \text{and } i \geq 2 \\ a_{ij} = 1 - \frac{T}{\Delta_i} v_i(k), & \text{if } i=j \\ a_{ij} = 0, & \text{otherwise} \end{cases} \qquad (7)$$

$$B = \begin{cases} b_{ij} = \frac{T}{\Delta_i}, & \text{if } i=1 \text{ and } j=1,2 \\ & \text{or } j-i=1 \text{ and } i \geq 2 \\ b_{ij} = 0, & \text{otherwise} \end{cases} \qquad (8)$$

$$u(k) = \begin{bmatrix} q_0(k) & r_1(k) - s_1(k) & \dots & r_N(k) - s_N(k) \end{bmatrix}^T \qquad (9)$$

$$C = \begin{bmatrix} 0 & \dots & 0 & 1 \end{bmatrix} \qquad (10)$$

with $v = [v_1 \ \dots \ v_N]^T \in \mathbb{R}^N$, $A \in \mathbb{R}^{N \times N}$, $B \in \mathbb{R}^{N \times (N+1)}$, where q_0 denotes the total flow of vehicles at the entry of the considered highway stretch and acts as an input to system (5), along with r_i and s_i; while v_i, $i = 1, \dots, N$, are viewed as time-varying parameters of system (5). The variable ρ_N at the exit of the considered highway stretch is viewed as the output of the system and may be obtained via $\rho_N = q_N / v_N$, using total flow measurements q_N at the exit of the considered stretch.

Before studying the observability of (5)–(10), we summarize the assumptions that guarantee that the matrix A is known as well as that the input u and output y are measured.

- The average speed of all vehicles at a segment of the highway equals the average speed of connected vehicles at the same segment, and hence, it can be obtained from regularly received messages by the connected vehicles. This assumption is indeed validated by use of real microscopic data in Section III-A.
- The total flow of vehicles at the entry and exit of the considered highway stretch, q_0 and q_N, respectively, are measured via conventional detectors.
- The total flow of vehicles at ramps, i.e., r_i and s_i, $i = 1, \dots, N$, are measured via conventional detectors.

The above formulation may be modified to incorporate different total flow measurement configurations. In Section IV we consider the case in which additional mainstream flow measurements (using conventional detectors) are employed to replace a corresponding number of flows at ramps.

B. Observability of the System

System (5) can be viewed as a known linear time-varying system. As it is stated in Section II-A, it is assumed that the quantities q_0, v_i, r_i, and s_i, for all i, are available, which implies that the matrix A and the input u in (5) may be calculated in real time. We show next that system (5)–(10) is observable at

$k = k_0 + N - 1$, for any initial time $k_0 \geq 0$. We construct the observability matrix

$$O(k_0, k_0 + N) = \begin{bmatrix} C \\ CA(v(k_0)) \\ CA(v(k_0+1)) A(v(k_0)) \\ \vdots \\ CA(v(k_0+N-2)) \cdots A(v(k_0)) \end{bmatrix}. \qquad (11)$$

From (7), A is lower triangular with non-zero entries only in the main diagonal and the first diagonal below it. Thus, from (10) it follows that $O \in \mathbb{R}^{N \times N}$ is an anti-lower triangular matrix, namely, a matrix with zero elements above the anti-diagonal, that is

$$O(k_0, k_0 + N) = \begin{bmatrix} 0 & \dots & 0 & 1 \\ 0 & \dots & o_{2,N-1} & \star \\ \vdots & \ddots & \star & \star \\ o_{N,1} & \star & \star & \star \end{bmatrix} \qquad (12)$$

where for all $2 \leq i \leq N$

$$o_{i,N-i+1} = \frac{T^{i-1}}{\Delta_N \cdots \Delta_{N-i+2}} \times \prod_{j=N-i+1}^{j=N-1} v_j(k_0+i+j-1-N). \qquad (13)$$

Therefore

$$|\det(O)| = \left| \prod_{j=2}^{j=N} o_{j,N-j+1} \right| \qquad (14)$$

and thus, relation $\det(O) \neq 0$ holds if the anti-diagonal elements of O are non-zero. Since v_i, $i = 1, \dots, N$, are lower and upper-bounded (and positive) for all times,[1] it follows using (13) that the matrix O is invertible, and thus, (5)–(10) is completely observable. Note that the measurement of ρ_N (or, equivalently, the measurement of q_N), rather than any other intermediate density, is necessary for system (5)–(10) to be observable. To see this, note that if

$$C = \begin{cases} c_{ij} = 1, & \text{if } i=1 \text{ and } j=J \\ c_{ij} = 0, & \text{otherwise} \end{cases} \qquad (15)$$

with $J < N$, then the $J+1, \dots, N$ columns of $O(k_0, k_0 + \bar{N})$ are zero for all $k_0 \geq 0$ and $\bar{N} \geq N$. Thus, the system cannot be observable. In other words, a fixed flow sensor should necessarily be placed at the last segment of the highway in order to guarantee density observability based on model (5)–(10).

C. Kalman Filter

We employ a Kalman filter for the estimation of the total density of vehicles on a highway (Fig. 1). Defining

---

[1]Note that the assumptions of lower and upper boundness of the average segment speeds trivially hold in a real traffic system (assuming that at each time instant and in every segment there is at least one vehicle with non-zero speed).

$\hat{x} = (\hat{\rho}_1, \ldots, \hat{\rho}_N)^T$, the Kalman filter's equations are (e.g., [3])

$$\hat{x}(k+1) = A\left(v(k)\right)\hat{x}(k) + Bu(k)$$
$$+ A\left(v(k)\right)K(k)\left(z(k) - C\hat{x}(k)\right) \quad (16)$$

$$K(k) = P(k)C^T\left(CP(k)C^T + R\right)^{-1} \quad (17)$$

$$P(k+1) = A\left(v(k)\right)\left(I - K(k)C\right)P(k)A\left(v(k)\right)^T + Q \quad (18)$$

where z is a noisy version of the measurement y, $R = R^T > 0$ and $Q = Q^T > 0$ are tuning parameters. Note that, in the ideal case in which there is additive, zero-mean Gaussian white noise in equations (5) and (6), respectively, R and Q represent the (ideally known) covariance matrices of the measurement and process noise, respectively. Since the system equations here are relatively complex, some tuning of R, Q may be needed for best estimation results. The initial conditions of the filter (16)–(18) are chosen as

$$\hat{x}(k_0) = \mu \quad (19)$$
$$P(k_0) = H \quad (20)$$

where μ and $H = H^T > 0$, which, in the ideal case in which $x(k_0)$ is a Gaussian random variable, represent the mean and auto covariance matrix of $x(k_0)$, respectively. The Kalman filter (16)–(20) delivers estimates of the total densities $\hat{\rho}_i$ as indicated at the output of the Kalman filter in Fig. 1.

In addition to guaranteeing observability of the system, we impose the conditions that the pair (A, C) is uniformly completely observable (UCO) and that the pair $\left(A, Q^{1/2}\right)$ is uniformly completely controllable (UCC), which, in combination with the fact that A is uniformly bounded with bounded from below positive determinant, assuming that $1 - (T/\Delta_i)v_i$, $\forall i$, are positive and bounded from below, guarantee that the homogenous part of the estimator is exponentially stable and that the covariance of the estimation error is bounded [23]. We show that (A, C) is UCO by showing that $\exists \epsilon_1, \epsilon_2 > 0$ such that

$$\epsilon_1 I_{N \times N} \le O^T(k_0, k_0+N)O(k_0, k_0+N) \le \epsilon_2 I_{N \times N}, \ \forall k_0 \ge 0. \quad (21)$$

Since O has the special form (12), i.e., it is an anti-lower triangular matrix with uniformly bounded from below and above, positive elements on the anti-diagonal, it follows that it has N independent columns, and hence

$$O^T(k_0, k_0 + N)O(k_0, k_0 + N) > 0, \quad \forall k_0 \ge 0. \quad (22)$$

Thus, relation (21) holds with

$$\epsilon_1 = \inf_{k_0 \ge 0} \lambda_{\min}\left(O^T(k_0, k_0 + N)O(k_0, k_0 + N)\right) \quad (23)$$

$$\epsilon_2 = \sup_{k_0 \ge 0} \lambda_{\max}\left(O^T(k_0, k_0 + N)O(k_0, k_0 + N)\right). \quad (24)$$

Note that $\epsilon_2 < \infty$ since A is bounded. Thus, since from (13), (14) it follows that $\det(O)^2$ is uniformly bounded from below, it follows that $\epsilon_1 > 0$.

TABLE I
PARAMETERS OF THE MODEL (1), (2), AND (25)

T	$\frac{1}{360}$ (h)	δ	1.4	Δ_i	0.5 (km)	N	20
v_f	120 $\left(\frac{\text{km}}{\text{h}}\right)$	τ	$\frac{1}{180}$ (h)	ρ_cr	33.5 $\left(\frac{\text{veh}}{\text{km}}\right)$		
ν	35 $\left(\frac{\text{km}^2}{\text{h}}\right)$	α	1.4324	κ	13 $\left(\frac{\text{veh}}{\text{km}}\right)$		

The fact that $(A, Q^{1/2})$ is UCC follows exploiting the choice $Q = \sigma I_{N \times N}$, for some bounded $\sigma > 0$, and the fact that A is lower triangular with bounded from below positive elements on the main diagonal.

III. EVALUATION OF THE PERFORMANCE OF THE ESTIMATOR BASED ON A METANET MODEL AS GROUND TRUTH

For preliminary assessment of the developed estimation scheme, we test in this section the performance of the Kalman filter employing the second-order METANET model [28] as ground truth. METANET employs equation (1) for the total density of vehicles together with (2) for the total flow. The average speed at segment i is given within METANET by

$$v_i(k+1) = v_i(k) + \frac{T}{\tau}\left(V\left(\rho_i(k)\right) - v_i(k)\right) + \frac{T}{\Delta_i}v_i(k)$$
$$\times\left(v_{i-1}(k) - v_i(k)\right) - \frac{\nu T}{\tau\Delta_i}\frac{\rho_{i+1}(k) - \rho_i(k)}{\rho_i(k) + \kappa}$$
$$- \frac{\delta T}{\Delta_i}\frac{r_i(k)v_i(k)}{\rho_i(k) + \kappa}, \quad i = 1, \ldots, N \quad (25)$$

with $v_0 = v_1$ and $\rho_N = \rho_{N+1}$, where the nominal average speed V is given by $V(\rho) = v_f e^{-1/\alpha(\rho/\rho_\text{cr})^\alpha}$, and $\tau, \nu, \kappa, \delta, v_f$, ρ_cr, α are positive model parameters. In particular, v_f denotes the free speed, ρ_cr the critical density, and α the exponent of the stationary speed equation. The METANET model parameters, taken from [45], are shown in Table I.

The measurements of the total flow of vehicles at the entry and exit of the highway stretch under consideration and the measurements of the total flow at the on-ramps or off-ramps are subject to additive measurement noise. Moreover, there is additive process noise affecting the speed and flow equations, namely, (2) and (25), respectively. The mean speed (of all vehicles) measurements, which stem from connected vehicles only, are also subject to additive noise, which represents the incurred inaccuracy due to penetration rates of connected vehicles lower than 100% at the specific highway segment; clearly, this results in an error of the measurement of the real all-vehicles average segment speed. In order to evaluate the effect of varying penetration rates of connected vehicles on the speed error we use real microscopic traffic data.

A. Specification of the Noise Statistics for the Speed Measurement Error Using Real Microscopic Traffic Data

We utilize here the real microscopic traffic data collected within the Next Generation SIMulation program [40] for computing the speed measurement error due to the presence of both
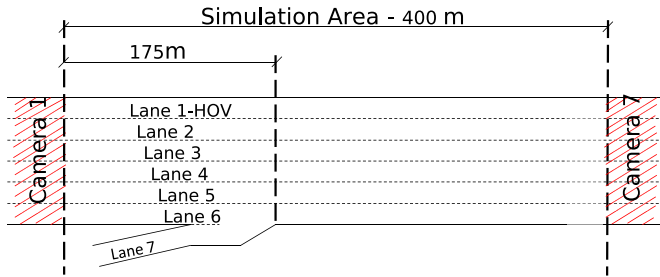
Fig. 2. Graphical representation of the stretch of Highway I-80 in Emeryville, California, related to the NGSIM data.

Fig. 3. Mean and standard deviation of the measurement speed error (in kilometers per hour) as the penetration rate of connected vehicles varies for the NGSIM data.

Fig. 4. Mean and standard deviation of the measurement speed error (in kilometers per hour) as the penetration rate of connected vehicles varies for the NGSIM data. When there is no available measurement stemming from connected vehicles, the missing measurement is replaced by the last reported speed value.

connected and conventional vehicles. Since these data incorporate non-negligible errors in the position of individual vehicles (see, e.g., [30]), correction methodologies are proposed in the literature to improve their reliability; in this work, we utilize the data processed by [20] and [21], which include the trajectories of all vehicles travelling along a stretch in the northbound direction of I-80 in Emeryville, California, recorded from 4:00 PM to 4:15 PM on April 13, 2005. The highway is composed of 6 lanes, where lane 1 is a so-called HOV (high-occupancy vehicle) lane, characterized by access restricted to a limited set of vehicles. Therefore, the HOV lane is excluded in the investigations to follow.

The considered stretch (sketched in Fig. 2) is 400 m long, and an on-ramp is entering the mainstream, with the merge nose located 175 m after the network origin. A strong congestion is present, with congestion waves coming from downstream and crossing the entire stretch.

Vehicles entering the stretch are randomly tagged as connected according to a uniform distribution, therefore the percentage effectively varies in time and space. All speed measurements, needed for the computation of the speed error, are extracted from the available trajectory data, see, e.g., [20]. In particular, we run 10 simulation replications, each time considering different sets of vehicles being connected (for a fixed penetration rate); in each replication, the speed error is computed every 10 s as the difference between the average speed of all vehicles and the average speed computed only using information from connected vehicles. The mean and standard deviation of the error are then computed by taking the average over the 10 simulation replications.

In Fig. 3, we display the mean and standard deviation of the error, i.e., of the difference between the actual average speed computed from the speeds of all vehicles and the "measured" average speed as reported by connected vehicles only, averaged over all time steps (in order to come up with a single value); against the penetration rate of connected vehicles. The error is computed considering only the time instances where there is at least one connected vehicle reporting its speed.

In fact, due to the low and time-varying penetration rates, the stretch may not contain any connected vehicle at some time instants. However, in order to run the estimator in real-time, a speed value for every segment is needed at every time step. A potential simple solution, in order to overcome these potential issues, is to feed the filter, whenever there is no speed information reported from connected vehicles, with the last
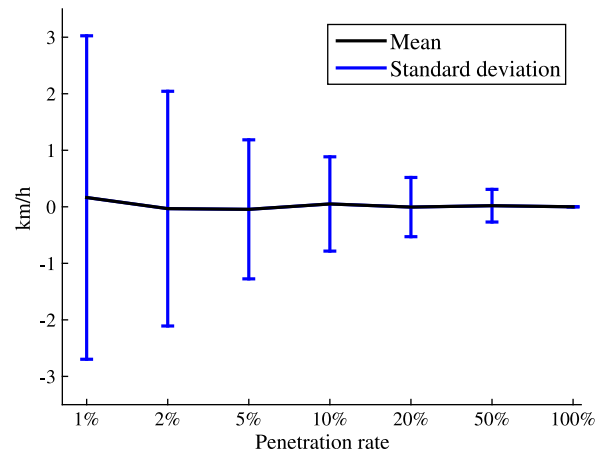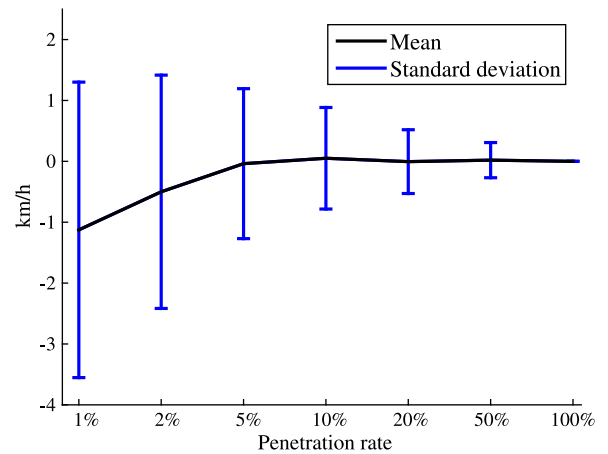
reported speed value that corresponds to a specific segment, see, e.g., [18]. Computing the speed error this way, results in a different speed error than the speed error computed previously by ignoring in the calculation any missing measurements. The error statistics for this case are shown in Fig. 4.

Comparing Fig. 3 with Fig. 4, one can observe that in the case where a missing speed measurement is replaced by the last reported speed value, there is a small decrease of the standard deviation, but also a small appearing bias between the speed reported from connected vehicles and the real speed. In both cases, the standard deviation of the error is very small even at very low penetration rates; and is reduced when the penetration rate of connected vehicles is increased. These results validate our initial assumption that the measured speed stemming from connected vehicles is sufficiently reliable even at low penetration rates; and provides a guide for the selection of the error statistics while designing the Kalman Filter.

TABLE II
MEASUREMENT NOISE γ_i^w AND PROCESS NOISE ξ_i^w, $i = 0, \ldots, N$
AFFECTING THE w VARIABLE AT SEGMENT i

	γ_i^q	γ_i^r	γ_i^s	γ_i^v	ξ_i^v	ξ_i^q
SD	$25\frac{\text{veh}}{\text{h}}$	$10\frac{\text{veh}}{\text{h}}$	$5\frac{\text{veh}}{\text{h}}$	$3\frac{\text{km}}{\text{h}}$	$5\frac{\text{km}}{\text{h}}$	$25\frac{\text{veh}}{\text{h}}$

TABLE III
PARAMETERS OF THE KALMAN FILTER (16)–(20) AND (7)–(10)

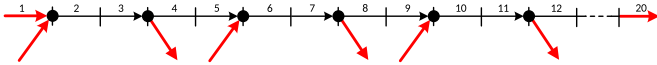| Q	R	μ	H
$I_{N \times N}$	100	$(15, \ldots, 15)^T$	$I_{N \times N}$

Fig. 5. Layout of the highway stretch considered in the simulation investigations in Section III. A red thick arrow indicates that a fixed flow sensor is placed at the exit of the corresponding highway segment or on-ramp or at the entry of the corresponding off-ramp.
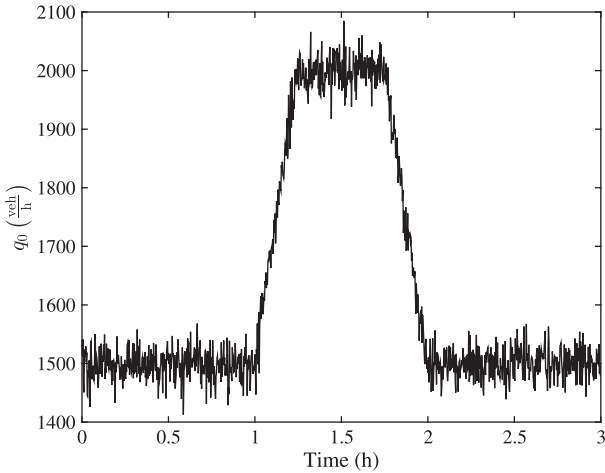

Fig. 6. Total flow of vehicles q_0 at the entry of the highway stretch under consideration.

B. Simulation Results

For the following simulation investigations, we use zero-mean (at the end of the section we consider also the case of additive speed measurement bias) Gaussian white noise with standard deviation (SD) shown in Table II. Comparing the value of the additive noise in the speed measurements γ_i^v in Table II with Fig. 3, we conclude that the simulation scenario presented below corresponds to approximately 1% of connected vehicles.

The utilized parameters and initial conditions of the Kalman filter (16)–(20), (7)–(10) are shown in Table III. In Fig. 6 we show the employed scenario of total input flow at the entry of the considered highway stretch, which is shown in Fig. 5, for our simulation investigation of a 20-segment highway stretch. We assume that there are three on-ramps at segments 2, 6, 10 with constant inflows satisfying $r_2 = r_6 = r_{10} = 150$ veh/h. Three off-ramps are supposedly present on the highway under study, specifically at segments 4, 8, 12. It is assumed that $s_i = 0.1q_{i-1}$, $i = 4, 8, 12$, i.e., the respective exit rates amount to 10%. The average speed at segment 2 (where the first on-ramp is located) is shown in Fig. 7. It is evident from Fig. 7 that a congestion is created between the first and second hour of our
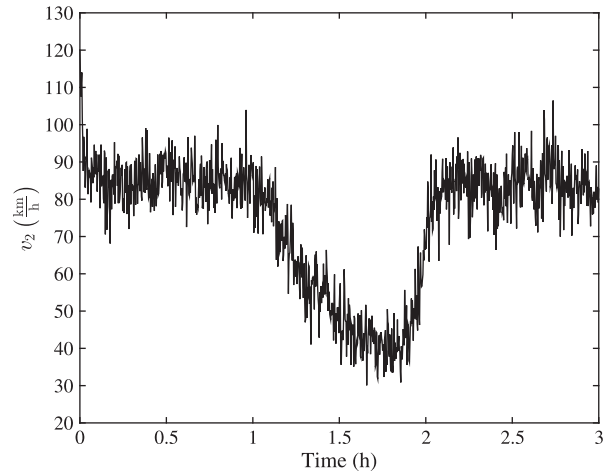

Fig. 7. Average speed v_2 on the second segment of the considered highway stretch as it is produced by the METANET model (1), (2), and (25), with parameters given in Table I and additive process noise given in Table II.
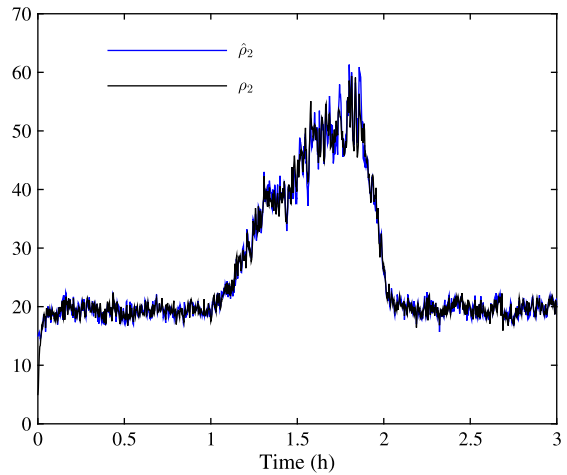

Fig. 8. Total density of vehicles ρ_2 (in vehicles per kilometer) on the second segment of the considered highway stretch (black line) as it is produced by the METANET model (1), (2), and (25), with parameters given in Table I and additive process noise given in Table II, and its estimate $\hat{\rho}_2$ (blue line) as it is produced by the Kalman filter (16)–(20) and (7)–(10), with parameters given in Table III.

test, whereas free-flow conditions are prevailing at the first and last hour. Congestion starts approximately at the location of the second on-ramp, i.e., at the sixth segment of the highway, and propagates backwards all the way to the input of the highway.

In both traffic conditions, our estimator successfully estimates the total density of vehicles on the highway, as it is evident from Figs. 8 and 9, which display the actual density and its estimate at two different segments of the highway, namely, at segments 2 (at which congested conditions prevail for one hour) and 8, respectively. Note the fast convergence of the produced density estimates, starting from remote initial values. Fig. 10 shows the relative performance index

$$P_R = \frac{\sqrt{\frac{1}{MN}\sum_{k=0}^{k=M}\sum_{i=1}^{i=N}\left(\rho_i(k) - \hat{\rho}_i(k)\right)^2}}{\frac{1}{MN}\sum_{k=0}^{k=M}\sum_{i=1}^{i=N}\rho_i(k)} \quad (26)$$
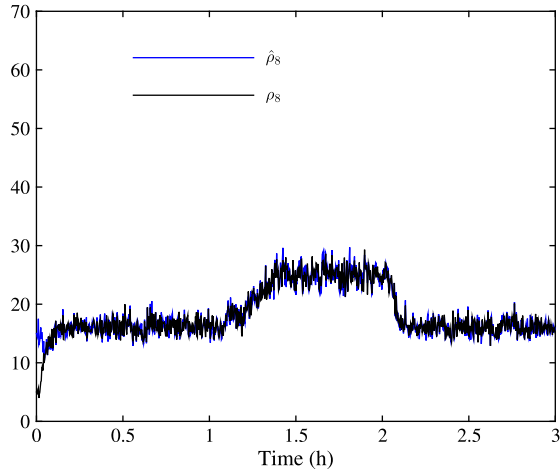
Fig. 9. Total density of vehicles ρ_8 (in vehicles per kilometer) on the eighth segment of the considered highway stretch (black line) as it is produced by the METANET model (1), (2), and (25), with parameters given in Table I and additive process noise given in Table II, and its estimate $\hat{\rho}_8$ (blue line) as it is produced by the Kalman filter (16)–(20) and (7)–(10), with parameters given in Table III.
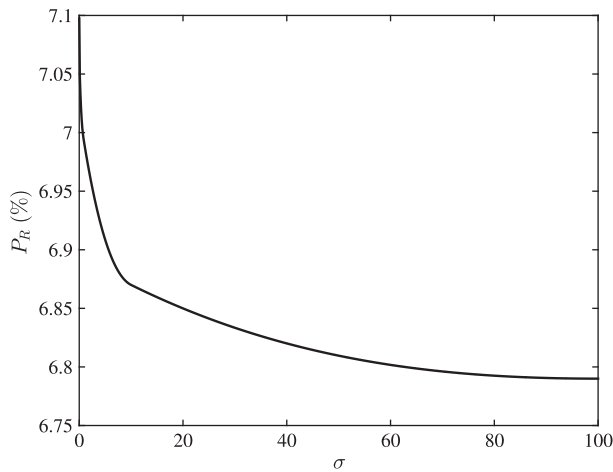

Fig. 10. Relative performance index P_R (in %) defined in (26) as a function of the tuning parameter $Q = \sigma I_{N \times N}$ of the Kalman filter (16)–(20) and (7)–(10), with parameters given in Table III.

of the estimation scheme, with simulation time horizon $M = 3/T = 1080$, as a function of the parameter $Q = \sigma I_{N \times N}$ of the Kalman filter while R was kept constant at a value $R = 100$. From Fig. 10 it is evident that the Kalman filter is robust to the choice of the tuning parameter Q. Note that, due to the effect of the initial error between the real and the estimated densities, the relative performance index takes larger values than when it is computed on a time interval after the initial transient period of the estimator's response.

We also evaluate the performance of the estimation scheme under delayed speed measurements coming from the connected vehicles. We assume that at each sampling step the information that is available to the estimator are speed measurements from the previous minute. We show in Fig. 11 the estimation of the density in the second segment when the estimator uses at each time step a simple moving average of the past six speed measurements, starting from the measurement of the previous time step. One can observe that the one-step delay has little
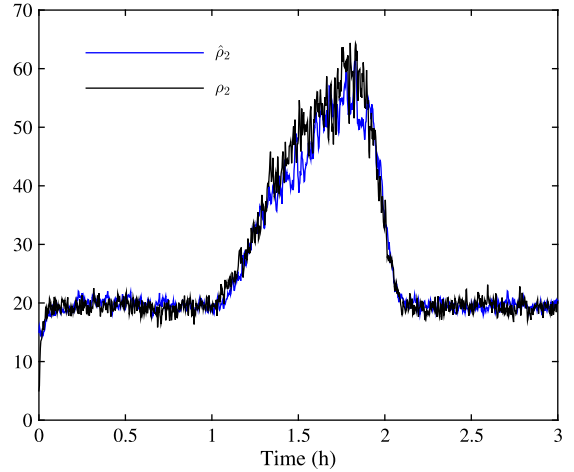

Fig. 11. Total density of vehicles ρ_2 (in vehicles per kilometer) on the second segment of the considered highway stretch (black line) and its estimate $\hat{\rho}_2$ (blue line) as it is produced by the Kalman filter (16)–(20) and (7)–(10), with parameters given in Table III, using a simple moving average, of the past six speed measurements starting from the measurement of the previous time step, instead of the current speed measurements.

effect on the estimation. In particular, the relative performance index (26) increases to a value of approximately 10% from a value about 7% in the delay-free case.

We also test the performance of the estimation scheme in the case in which at some time instances there is no speed information reported by connected vehicles. A simple procedure to overcome this difficulty is to replace the missing speed information with the last reported speed value, see, e.g., [18]. Applying this procedure to the computation of the speed error for the NGSIM data, we get a biased speed error, as shown in Fig. 4. To emulate this situation, we choose for the speed measurement error a Gaussian noise with mean -1 km/h and standard deviation 2.5 km/h, which corresponds, according to Fig. 4, to a penetration rate of approximately 1%. In Fig. 12, we display the real and estimated density at segments 2 and 8 for this case. The performance index has a value about 7% and the estimation is slightly biased.

IV. TRAFFIC ESTIMATION FOR UNMEASURED TOTAL FLOW AT ON-RAMPS AND OFF-RAMPS

A. Model Derivation and Its Observability Properties

In the case that the total flow at some on-ramps or off-ramps is not directly measured, we treat these flows as additional unmeasured states to be estimated by a Kalman filter. Hence, we augment the state (4) as

$$\bar{x} = (\rho_1, \ldots, \rho_N, \theta_1, \ldots, \theta_{l_r + l_s})^T \qquad (27)$$

where l_r and l_s are the number of unmeasured flows at on-ramps and off-ramps, respectively, and $\theta_i = \begin{cases} \frac{T}{\Delta_i} r_{n_i}, & \text{if } n_i \in L_r \\ \frac{T}{\Delta_i} s_{n_i}, & \text{if } n_i \in L_s \end{cases}$,

for all $i = 1, \ldots, l_r + l_s$, with $L_r = \{n_1, \ldots, n_{l_r}\}$ and $L_s = \{n_{l_r+1}, \ldots, n_{l_r+l_s}\}$, being the collection of segments, denoted by n_i, which have an on-ramp and an off-ramp, respectively, whose flows are not directly measured. Assuming that at a segment i there can be either only one on-ramp or only one
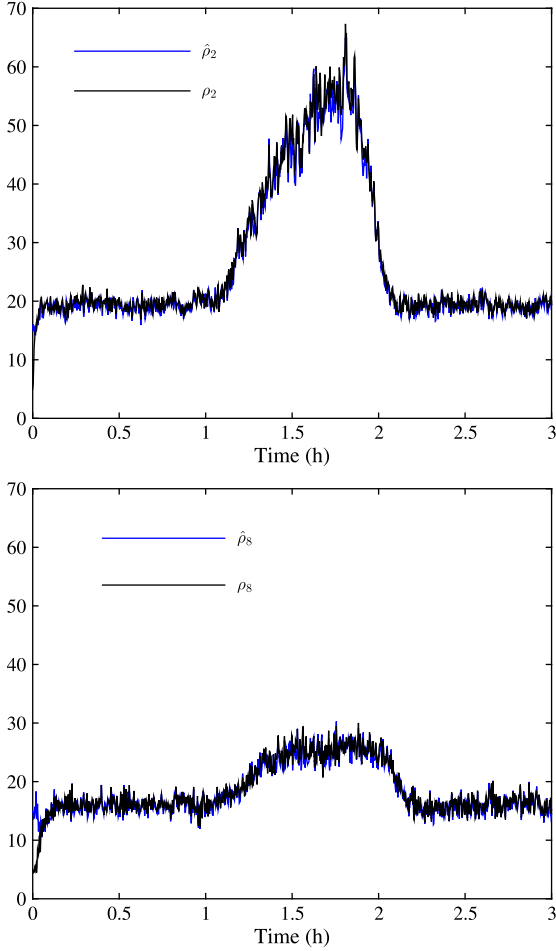
Fig. 12. Total density of vehicles ρ_2 and ρ_8 (in vehicles per kilometer) on the second and eighth segments of the considered highway stretch (black line) as it is produced by the METANET model (1), (2), and (25), with parameters given in Table I and additive process noise given in Table II, where the measurement noise of the speed has bias of -1.5 km/h and a standard deviation of $\gamma_i^v = 3.5$ km/h, and their estimates $\hat{\rho}_2$ and $\hat{\rho}_8$ (blue line) as they are produced by the Kalman filter (16)–(20) and (7)–(10), with parameters given in Table III.

off-ramp (which is typically the case on a highway) and that the unmeasured on-ramp and off-ramp flows are constant (or, effectively, slowly varying), the unmeasured ramp flow dynamics may be reflected by a random walk, i.e., $\theta_i(k+1) = \theta_i(k) + \xi_i^\theta(k)$, where ξ_i^θ is zero-mean white Gaussian noise. Thus, the deterministic part of the dynamics of the total density given in (1) and of θ_i are

$$\bar{x}(k+1) = \bar{A}\left(v(k)\right)\bar{x}(k) + \bar{B}\bar{u}(k) \tag{28}$$

where

$$\bar{A}\left(v(k)\right) = \begin{cases} \bar{a}_{ij} = \frac{T}{\Delta_i} v_{i-1}(k), & \text{if } i - j = 1 \\ & \text{and } i \geq 2 \\ \bar{a}_{ij} = 1 - \frac{T}{\Delta_i} v_i(k), & \text{if } i = j \\ \bar{a}_{n_i j} = 1, & \text{if } n_i \in L_r \\ & \text{and } j = N + i \\ \bar{a}_{n_i j} = -1, & \text{if } n_i \in L_s \\ & \text{and } j = N + i \\ \bar{a}_{ij} = 1, & \text{if } N < i \leq N_1 \\ & \text{and } j = i \\ \bar{a}_{ij} = 0, & \text{otherwise} \end{cases} \tag{29}$$

$$\bar{B} = \begin{bmatrix} \bar{b}_{ij} = \frac{T}{\Delta_i}, & \text{if } i = 1 \text{ and } j = 1 \\ \bar{b}_{m_i j} = \frac{T}{\Delta_{m_i}}, & \text{if } m_i \notin \bar{L}, 1 \leq m_i \leq N, \\ & 1 \leq i \leq N_2, \text{ and } j = i + 1 \\ \bar{b}_{ij} = 0, & \text{otherwise} \end{bmatrix} \tag{30}$$

$$\bar{u}(k) = \begin{bmatrix} \bar{u}_i = q_0(k), & \text{if } i = 1 \\ \bar{u}_{i+1} = r_{m_i} - s_{m_i}, & \text{if } m_i \notin \bar{L} \end{bmatrix} \tag{31}$$

with $\bar{L} = L_r \cup L_s$, $N_1 = N + l_r + l_s$, $N_2 = N - l_r - l_s$, $\bar{A} \in \mathbb{R}^{N_1 \times N_1}$, $\bar{B} \in \mathbb{R}^{N_1 \times (N_2+1)}$.

We now turn our attention to the measured outputs for the present case, where some on-ramp or off-ramp flows are not measured. If there is exactly one unmeasured ramp within the considered highway stretch, then no additional measurements are necessary. On the other hand, if there are more than one unmeasured ramps within the stretch, we need one mainstream flow measurement at any highway segment between every two consecutive unmeasured ramps.

In summary, the measured outputs associated with system (28)–(31) are the density (or, equivalently, the flow) at the exit of the considered highway stretch and at a highway segment between every two consecutive ramps whose flows are not measured. Therefore

$$\bar{y}(k) = \bar{C}\bar{x}(k) \tag{32}$$

where $\bar{C} \in \mathbb{R}^{(l_r+l_s) \times (N+l_r+l_s)}$ is defined as

$$\bar{C} = \begin{bmatrix} \bar{c}_{ij} = 1, & \text{for all } i = 1, \ldots, l_r + l_s - 1 \\ & \text{and some } n_i^* \leq j \leq n_{i+1}^* - 1 \\ \bar{c}_{ij} = 1, & \text{if } i = l_r + l_s \text{ and } j = N \\ \bar{c}_{ij} = 0, & \text{otherwise} \end{bmatrix} \tag{33}$$

where $\bar{L}^* = \{n_1^*, n_2^*, \ldots, n_{l_r+l_s}^*\}$ is the set $\bar{L}$ ordered by $<$.

Although it is physically intuitive that (28)–(33) is observable when additional mainstream fixed flow sensors are placed at some segment between every two consecutive unmeasured ramps, we prove in Appendix A that the system is observable when a fixed sensor is placed on the mainstream at every segment immediately before an unmeasured ramp, i.e., when $\bar{y}$ in (32) satisfies $\bar{y}_{l_r+l_s+1} = \rho_N$ and $\bar{y}_j = \rho_{n_j-1}$, $n_j \in \bar{L}^*$. The reason is that since system (28)–(33) is time-varying with a large number of states and, potentially, outputs, an analytical observability study considering every possible sensor configuration requires lengthy calculations that would distract the reader from the main ideas and results of the present section, namely, traffic state estimation in the case of unmeasured ramps.

B. Kalman Filter Design and Evaluation of Its Performance

We employ the Kalman filter (16)–(20) with parameters given in Table IV (in particular, the $\bar{q}_{N+iN+i}$ elements of $\bar{Q}$ represent the filter's anticipation for the covariance of ξ_i^θ), for the estimation of the state $\bar{x}$, defined in (27), of system (28)–(33). We assess the filter's performance, employing the

TABLE IV
PARAMETERS OF THE KALMAN FILTER EMPLOYED IN SECTION IV

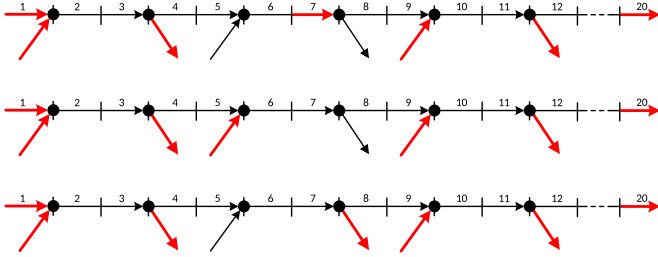| $\bar{Q}$	$\bar{R}$	$\bar{\mu}$	$\bar{H}$
$I_{(N+2)\times(N+2)}$	$100 I_{2\times 2}$	$(2,\dots,2)^T$	$I_{(N+2)\times(N+2)}$

Fig. 13. Layouts of the highway stretches considered in the simulation investigations in Section IV for detector configurations A (top plot), B (middle plot), and C (bottom plot). A red thick arrow indicates that a fixed flow sensor is placed at the exit of the corresponding highway segment or on-ramp or at the entry of the corresponding off-ramp.
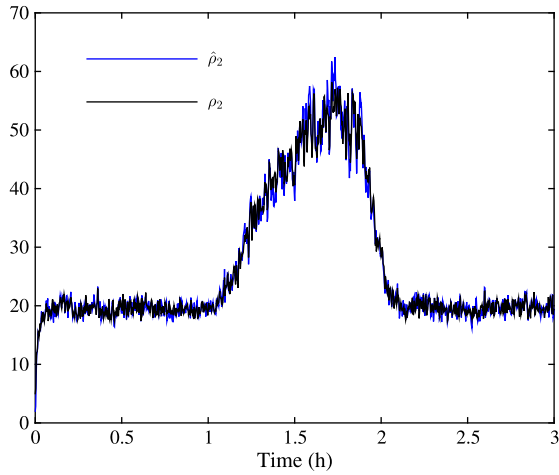

Fig. 14. Total density of vehicles ρ_2 (in vehicles per kilometer) on the second segment of the considered highway stretch (black line) and its estimate $\hat{\rho}_2$ (blue line) as it is produced by the Kalman filter with parameters $\bar{Q} = \text{diag}(I_{N\times N}, 0.025)$, $\bar{R} = 100$, $\bar{\mu} = (2,\dots,2)^T$, and $\bar{H} = I_{(N+1)\times(N+1)}$, for the fixed sensor configuration C.
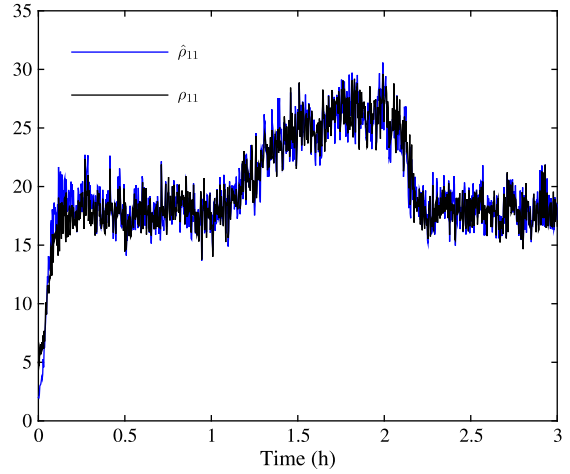

Fig. 15. Total density of vehicles ρ_{11} (in vehicles per kilometer) on the eleventh segment of the considered highway stretch (black line) and its estimate $\hat{\rho}_{11}$ (blue line) as it is produced by the Kalman filter with parameters $\bar{Q} = \text{diag}(I_{N\times N}, 0.025)$, $\bar{R} = 100$, $\bar{\mu} = (2,\dots,2)^T$, and $\bar{H} = I_{(N+1)\times(N+1)}$, for the fixed sensor configuration C.
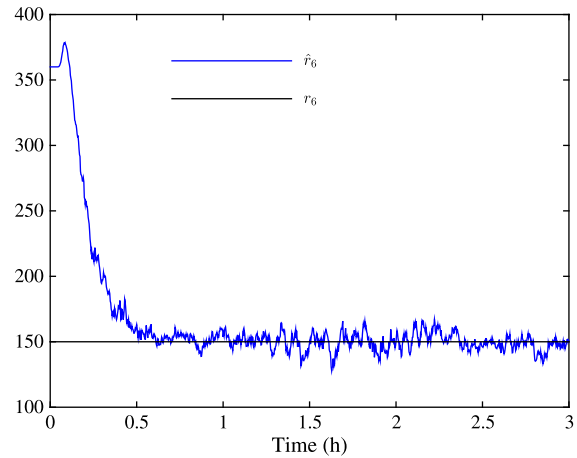

Fig. 16. Total flow of vehicles r_6 (in vehicles per kilometer) at the on-ramp located on the sixth segment of the considered highway stretch (black line) and its estimate $\hat{r}_6$ (blue line) as it is produced by the Kalman filter with parameters $\bar{Q} = \text{diag}(I_{N\times N}, 0.025)$, $\bar{R} = 100$, $\bar{\mu} = (2,\dots,2)^T$, and $\bar{H} = I_{(N+1)\times(N+1)}$, for the fixed sensor configuration C.

same scenario with the one considered in Section III, in the following different fixed detector configurations (see Fig. 13):

A. The total flow at on-ramp 6 and the total flow at off-ramp 8 are not measured. One additional mainstream total flow measurement is available from a fixed detector that is placed at the exit of the seventh segment.
B. The flow at off-ramp 8 is not measured, while all other ramp flows are measured by fixed flow detectors.
C. The flow at on-ramp 6 is not measured, while all other ramp flows are measured by fixed flow detectors.

For case C, we show in Figs. 14–16 the estimation of the density at segments 2, 11, and of the flow at on-ramp 6, respectively. We omit to show the estimation results for cases A and B because they are very similar to case C.

Note that, although in Section II-B we prove that (5)–(10) is observable when all on-ramp and off-ramp flows are measured, Figs. 14–16 suggest that (28)–(33) may also be observable

when a ramp is not measured and no additional mainstream flow measurement is available. However, an observability study in this case, employing the time-varying model (28)–(33), leads to complicated sufficient observability conditions that lack a clear physical meaning.

Finally, employing similar arguments to Sections II-C and IV-A it is shown that the pairs $(\bar{A}, \bar{C})$ and $(\bar{A}, \bar{Q}^{1/2})$ are UCO and UCC, respectively, and hence, the Kalman filter is exponentially stable.

V. ALTERNATIVE: TRAFFIC STATE ESTIMATION VIA ESTIMATION OF THE PERCENTAGE OF CONNECTED VEHICLES

In the present section we employ a Kalman filter for estimation of the percentage of connected vehicles, with respect

to the total number of vehicles. This estimation approach is an alternative to the one presented in previous sections. It does not need segment speed measurements, as in previous sections, but employs instead densities and flows of connected vehicles, which may be readily derived from presence reports of connected vehicles.

In principle, the alternative estimation approach may be employed if the density and flow measurements for connected vehicles feature sufficiently lower measurement error compared to the speed measurements. Furthermore, the additional information utilized by the alternative estimation scheme (and which is anyway available to the traffic monitoring and control unit, since these measurements are coming from connected vehicles) could potentially result in a more efficient traffic state estimation. Finally, the two approaches may even be combined towards a better estimation outcome, exploiting all available information coming from connected vehicles.

A. Model Derivation for the Percentage of Connected Vehicles

In accordance with (1) for the dynamics of the total density, the dynamics of the density ρ^a of connected vehicles are

$$\rho_i^a(k+1) = \rho_i^a(k) + \frac{T}{\Delta_i}\left(q_{i-1}^a(k) - q_i^a(k) + r_i^a(k) - s_i^a(k)\right) \tag{34}$$

where q_i^a is the flow of the connected vehicles at segment i; r_i^a and s_i^a are the corresponding inflow and outflow of connected vehicles at ramps. Define the inverse of the percentage of the connected vehicles at segment i of the highway as $\bar{p}_i$, i.e.,

$$\bar{p}_i = \frac{\rho_i}{\rho_i^a}. \tag{35}$$

Assuming that the average speed of conventional vehicles at a segment i equals the average speed of connected vehicles in the same segment, namely v_i, we get that

$$\bar{p}_i = \frac{\rho_i}{\rho_i^a} = \frac{q_i}{q_i^a} \tag{36}$$

where we used (2) and, accordingly, for connected vehicles

$$q_i^a = \rho_i^a v_i. \tag{37}$$

Using (1), (34), and (36) we get from (35) that

$$\bar{p}_i(k+1) = \frac{\left(\rho_i^a(k) - \frac{T}{\Delta_i}q_i^a(k)\right)\bar{p}_i(k) + \frac{T}{\Delta_i}q_{i-1}^a(k)\bar{p}_{i-1}(k)}{g_i^a(k)}$$

$$+ \frac{T}{\Delta_i}\frac{(r_i(k) - s_i(k))}{g_i^a(k)} \tag{38}$$

$$g_i^a(k) = \rho_i^a(k) + \frac{T}{\Delta_i}\left(q_{i-1}^a(k) - q_i^a(k) + r_i^a(k) - s_i^a(k)\right) \tag{39}$$

$i = 1, \ldots, N$. Defining the state

$$x^* = (\bar{p}_1, \ldots, \bar{p}_N)^T \tag{40}$$

we re-write (38) as

$$x^*(k+1) = A^*\left(q^a(k), \rho^a(k), r^a(k), s^a(k)\right)x^*(k)$$
$$+ B^*\left(q^a(k), \rho^a(k), r^a(k), s^a(k)\right)u^*(k) \tag{41}$$

$$y^*(k) = C^*x^*(k) \tag{42}$$

where

$$A^* = \begin{cases} a_{ij}^* = \frac{T}{\Delta_i}\frac{q_{i-1}^a(k)}{g_i^a(k)}, & \text{if } i - j = 1 \\ & \text{and } i \geq 2 \\ a_{ij}^* = \frac{\rho_i^a(k) - \frac{T}{\Delta_i}q_i^a(k)}{g_i^a(k)}, & \text{if } i = j \\ a_{ij}^* = 0, & \text{otherwise} \end{cases} \tag{43}$$

$$B^* = \begin{cases} b_{ij}^* = \frac{T}{\Delta_i}\frac{1}{g_1^a(k)}, & \text{if } i = 1 \\ & \text{and } j = 1, 2 \\ b_{ij}^* = \frac{T}{\Delta_i}\frac{1}{g_i^a(k)}, & \text{if } j - i = 1 \\ b_{ij}^* = 0, & \text{otherwise} \end{cases} \tag{44}$$

$$u^* = \begin{bmatrix} q_0(k) \\ r_1(k) - s_1(k) \\ \vdots \\ r_N(k) - s_N(k) \end{bmatrix} \tag{45}$$

$$C^* = \begin{bmatrix} 0 & \ldots & 0 & 1 \end{bmatrix} \tag{46}$$

$q^a = [q_0^a \ \ldots \ q_N^a]^T$, $\rho^a = [\rho_1^a \ \ldots \ \rho_N^a]^T$, $r^a = [r_1^a \ \ldots \ r_N^a]^T$, $s^a = [s_1^a \ \ldots \ s_N^a]^T$ and g_i^a, $i = 1, \ldots, N$, are defined in (39). Note that the variables r_i^a, s_i^a, ρ_i^a, and q_i^a are viewed as time-varying parameters of system (41). Finally, the variable $\bar{p}_N$ is viewed as output and may be obtained via $\bar{p}_N = q_N/q_N^a$, using total flow measurements q_N at the exit of the considered highway stretch.

B. Kalman Filter Design and Evaluation of Its Performance

Under an extra assumption (that guarantees that the matrices (43) and (44) are known, and that the input (45) and output (42) are measured), in comparison to Section II-A, namely, that the segment flows and densities of connected vehicles, q_i^a, $i = 0, \ldots, N$, and ρ_i^a, $i = 1, \ldots, N$, respectively, as well as the flows of connected vehicles at on-ramps and off-ramps, r_i^a and s_i^a, $i = 1, \ldots, N$, respectively, may be obtained from regularly received messages by the connected vehicles, it can be shown (see also [5]) that system (41)–(46) is observable utilizing identical arguments to Section II-B since $C = C^*$ and since the matrix A^* defined in (43) has the same structure with the matrix A defined in (7) and its elements a_{ij}^*, for $i - j = 1$, are positive as well as bounded from below and above.

We employ next the Kalman filter (16)–(20) with parameters given in Table V for the estimation of the state x^*, defined in (40), of system (41), (42). Note that since $C = C^*$ and since A^* in (43) has the same structure with the matrix A defined in (7) with bounded from below and above positive elements, exponential stability of the Kalman filter follows employing identical arguments to Section II-C and exploiting the choice $Q^* = \sigma^* I_{N \times N}$, for some bounded $\sigma^* > 0$.

TABLE V
PARAMETERS OF THE KALMAN FILTER EMPLOYED IN SECTION V

Q^*	R^*	μ^*	H^*
$I_{N \times N}$	100	$(10, \ldots, 10)^T$	$I_{N \times N}$

TABLE VI
MEASUREMENT NOISE γ_i^w AND PROCESS NOISE ξ_i^w, $i = 0, \ldots, N$
AFFECTING THE w VARIABLE AT SEGMENT i

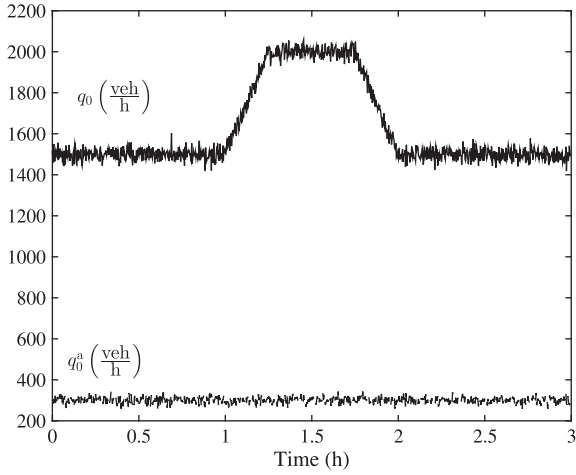|	γ_i^q	γ_i^r	γ_i^s	$\xi_i^{q^a}$	ξ_i^v	ξ_i^q
SD	$25 \frac{\text{veh}}{\text{h}}$	$10 \frac{\text{veh}}{\text{h}}$	$5 \frac{\text{veh}}{\text{h}}$	$15 \frac{\text{veh}}{\text{h}}$	$5 \frac{\text{km}}{\text{h}}$	$25 \frac{\text{veh}}{\text{h}}$

Fig. 17. Total flow of vehicles q_0 and the flow of connected vehicles q_0^a at the entry of the considered highway stretch.
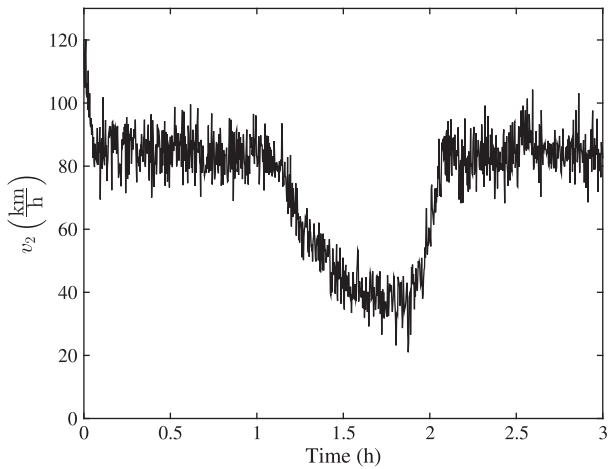

Fig. 18. Average speed v_2 on the second segment of the considered highway stretch as it is produced by the METANET model (1), (2), and (25), with parameters given in Table I and additive process noise given in Table VI.

We validate the performance of the Kalman filter employing as ground truth equations (1) and (34) for the total density of the vehicles and the density of connected vehicles, respectively, together with relations (2) and (37) for the total flow and the flow of connected vehicles, respectively. The average speed at segment i is given by (25). The noise statistics used in the simulations are shown in Table VI.

In Fig. 17 we show the employed scenario of input flow of connected vehicles and total input flow at the entry of the considered highway stretch for our simulation investigation.
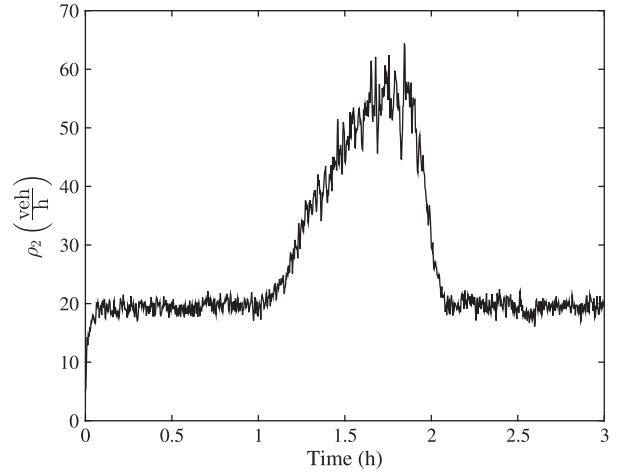

Fig. 19. Total density of vehicles ρ_2 on the second segment of the considered highway stretch as it is produced by the METANET model (1), (2), and (25), with parameters given in Table I and additive process noise given in Table VI.
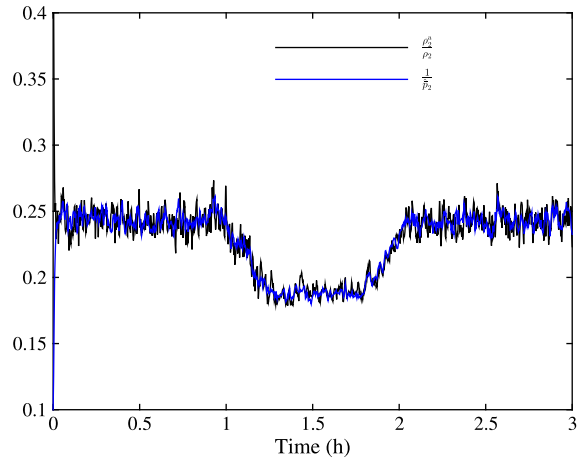

Fig. 20. Percentage of connected vehicles ρ_2^a/ρ_2 on the second segment of the considered highway stretch (black line) and its estimate $1/\hat{\bar{p}}_2$ (blue line) as it is produced by the Kalman filter, with parameters given in Table V.

We assume that the total flow and the flow of connected vehicles at on-ramps are $r_i = 150$ veh/h and $r_i^a = 100$ veh/h, $i = 2, 6, 10$, respectively. At off-ramps it is assumed that $s_i = 0.1 q_{i-1}$ and $s_i^a = 0.1 q_{i-1}^a$, $i = 4, 8, 12$. The average speed at segment 2 and the corresponding total density of vehicles are shown in Figs. 18 and 19, respectively. It is clear that congestion as well as free-flow conditions are reported, similarly to Section III. Our estimator successfully estimates the percentage of connected vehicles on the highway, as it is evident from Figs. 20 and 22 that display the actual percentage and its estimate at segments 2 and 8 of the highway stretch, respectively. Figs. 21 and 23 display the resulting estimation of the total density at segments 2 and 8, respectively, using relation (36).

The remarks on the robustness of the filter to delayed measurements coming from connected vehicles as well as to variations of the tuning parameters Q and R, for the case of the density estimator, apply mutatis mutandis to the case of the percentage estimator. Also, the estimation scheme presented in this section can be modified to incorporate additional mainstream total flow measurements, replacing a corresponding number of unmeasured ramp flows, in analogy with Section IV.
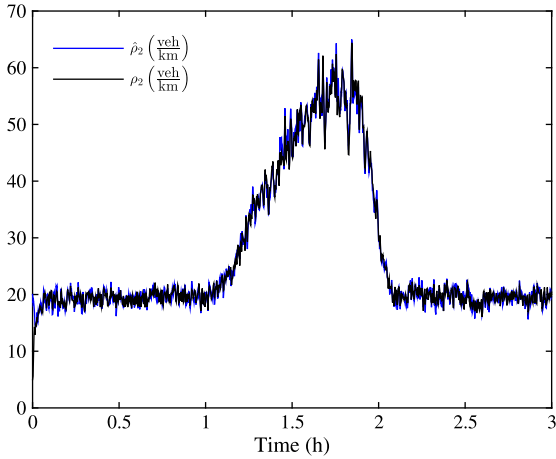
Fig. 21. Total density of vehicles ρ_2 on the second segment of the considered highway stretch (black line) and its estimate $\hat{\rho}_2 = \rho_2^a \hat{\bar{p}}_2$ (blue line) as it is produced by the Kalman filter, with parameters given in Table V.
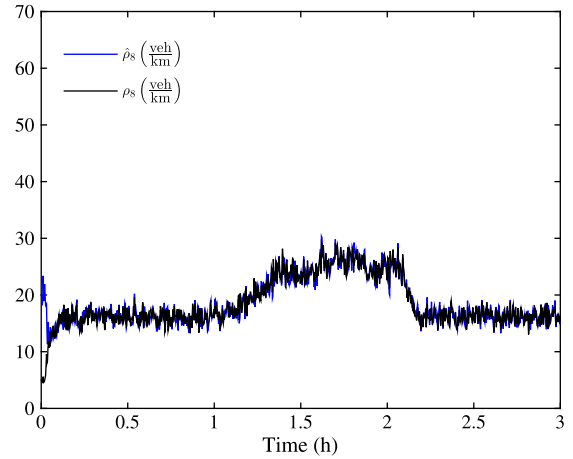

Fig. 23. Total density of vehicles ρ_8 on the eighth segment of the considered highway stretch (black line) and its estimate $\hat{\rho}_8 = \rho_8^a \hat{\bar{p}}_8$ (blue line) as it is produced by the Kalman filter, with parameters given in Table V.
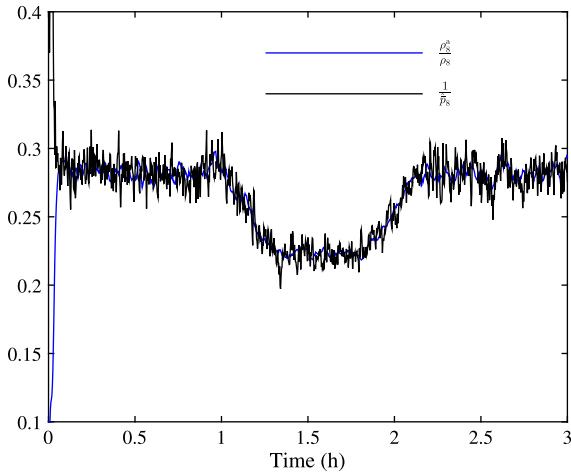

Fig. 22. Percentage of connected vehicles ρ_8^a / ρ_8 on the eighth segment of the considered highway stretch (black line) and its estimate $1/\hat{\bar{p}}_8$ (blue line) as it is produced by the Kalman filter, with parameters given in Table V.

VI. DISCUSSION AND CONCLUSION

The conclusions can be summarized as follows: i) We developed a) a traffic state estimation methodology for mixed traffic, i.e., traffic comprising both conventional and connected vehicles, utilizing only average speed measurements reported by connected vehicles and a minimum number of fixed detectors; and b) an alternative traffic state estimation methodology for mixed traffic, utilizing only flow and density measurements reported by connected vehicles together with a minimum number of fixed detectors (see also next paragraph). ii) It was demonstrated in simulation (employing also a suitable performance index) that for various traffic conditions (in particular, for both free-flow and congested conditions) and under the effect of noise or delay affecting the measurements utilized by the estimator, the developed estimation scheme successfully estimates the total density of vehicles on highways and that the produced density estimates converge very fast to the actual densities, starting from remote initial values. iii) It was

further demonstrated numerically that the developed estimation scheme has low sensitivity to certain tuning parameters. iv) Finally, analytical conditions for the observability of the system were derived under various measurement configurations, as along with conditions guaranteeing the exponential stability of the estimator.

One might raise the question of performance comparison between the two alternative estimation schemes. The two approaches have similarities since the linear parameter-varying models utilized in both estimation approaches are derived from the conservation law equation, in both approaches a Kalman filter is employed, and the same fixed flow measurements are used in both estimation schemes. However, the percentage estimator utilizes measurements of flow and density stemming from connected vehicles, as well as of inflow and outflow of connected vehicles at on-ramps and off-ramps, respectively. Since these measurements are coming from connected vehicles they are known to the MCU, similarly to the case of speed measurements used by the density estimator. Therefore, a fair performance comparison between the two estimation schemes would take into account the accuracy of the various measurements stemming from connected vehicles. For this reason, a subject of our ongoing research is the validation of the developed traffic estimation methodologies with a much more detailed microscopic simulation platform; considering a more realistic simulation of all involved real-time measurements.

Another topic of ongoing research is the validation of the developed schemes for various penetration rates of connected vehicles, by utilizing either real data or, by performing simulation experiments using a microscopic platform. In particular, studying the behavior of the estimation error with real data as the penetration rate of connected vehicles varies and using a microscopic simulation platform for testing the developed schemes in cases of mixed traffic for which there are no data available, such as, for instance, when traffic comprises both conventional vehicles and vehicles equipped with an Adaptive Cruise Control (ACC) system.

Future research will address the problem of optimal fixed sensor placement on highways via the optimization of certain

observability metrics. Since the models employed in this paper, for estimation purposes, are time-varying, due to their dependency on the traffic state of connected vehicles, an analytical study of the optimization of such metrics would be non-trivial. It is likely that the problem would be approached numerically considering various traffic conditions.

APPENDIX A

Observability of the System for the Case of Unmeasured Ramps

Assume the availability of $N+1$ measurements, i.e., for $k = k_0, \ldots, k_0 + N$ of the output ρ_N, (which implies that q_N is available), inputs q_0, r_i, and s_i, $i = 1, \ldots, N$ such that $i \notin \bar{L}$, and parameters v_i, $i = 1, \ldots, N$. Since the measured inputs do not affect the observability properties of the system, we assume henceforth, without loss of generality, that they are zero. In addition, whether the lack of a measurement concerns an on-ramp or an off-ramp at a given segment does not affect the observability properties of the system either. Hence, we assume that there are only unmeasured on-ramps, i.e., $l_s = 0$. For reducing the notational burden, we also impose $\Delta_j = \Delta$, $\forall j$. One can then uniquely determine $\rho_j(k)$, for all $k_0 \leq k \leq k_0 + j$ and $n_{l_r} \leq j \leq N - 1$ by recursively applying relation

$$\rho_j(k) = \frac{\Delta}{T v_j(k)} \rho_{j+1}(k+1) - \frac{\Delta}{T v_j(k)}$$
$$\times \left(1 - \frac{T}{\Delta} v_{j+1}(k)\right) \rho_{j+1}(k) \quad \text{(A.1)}$$

which follows from (3), starting at $j = N - 1$ and using measurements of the output $\bar{y}_{l_r+1}(k) = \rho_N(k)$, $k = k_0, \ldots, k_0 + N$. Setting $j = n_{l_r}$ in (3) we get that

$$r_{n_{l_r}}(k) = -v_{n_{l_r}-1}(k)\rho_{n_{l_r}-1}(k) + \frac{\Delta}{T}\rho_{n_{l_r}}(k+1)$$
$$- \frac{\Delta}{T}\left(1 - \frac{T}{\Delta}v_{n_{l_r}}(k)\right)\rho_{n_{l_r}}(k) \quad \text{(A.2)}$$

which also holds for $n_{l_r} = N$. Hence, the on-ramp flow $r_{n_{l_r}}(k)$ can be uniquely determined for $k = k_0, \ldots, k_0 + n_{l_r} - 1$ assuming mainstream measurements $\bar{y}_{l_r}(k) = \rho_{n_{l_r}-1}(k)$, $k = k_0, \ldots, k_0 + n_{l_r} - 1$. Employing (A.1) for all $n_{l_r-1} \leq j \leq n_{l_r} - 2$ and using the measurements $\rho_{n_{l_r}-1}(k)$, $k = k_0, \ldots, k_0 + n_{l_r} - 1$, $\rho_j(k)$ for all $n_{l_r-1} \leq j \leq n_{l_r} - 2$ and $k = k_0, \ldots, k_0 + j$ is uniquely determined (if $j = n_{l_r-1} = n_{l_r} - 1$ then ρ_j is directly measured). Assuming that $\bar{y}_{l_r-1}(k) = \rho_{n_{l_r-1}-1}(k)$, $k = k_0, \ldots, k_0 + n_{l_r-1} - 1$, is measured, it follows that $r_{n_{l_r-1}}(k)$, $k = k_0, \ldots, k_0 + n_{l_r-1} - 1$, is uniquely determined from (A.2) with $l_r \rightarrow l_r - 1$. Continuing this procedure up to $j = 1$ and n_1, it is shown that the system is observable at $k = k_0 + N$, $\forall k_0 \geq 0$. Similarly, it is shown that the system is observable in the case of exactly one unmeasured ramp, when a fixed flow sensor is placed on the mainstream at the segment immediately before the unmeasured ramp.

REFERENCES

[1] L. Alvarez-lcaza, L. Munoz, X. Sun, and R. Horowitz, "Adaptive observer for traffic density estimation," in *Proc. IEEE ACC*, Boston, MA, USA, 2004, pp. 2705–2710.

[2] A. Anand, G. Ramadurai, and L. Vanajakshi, "Data fusion-based traffic density estimation and prediction," *J. Intell. Transp. Syst.*, vol. 18, no. 4, pp. 367–378, 2014.

[3] B. D. O. Anderson and J. B. Moore, *Optimal Filtering*. Englewood Cliffs, NJ, USA: Prentice-Hall, 1979.

[4] V. Astarita, R. L. Bertini, S. d'Elia, and G. Guido, "Motorway traffic parameter estimation from mobile phone counts," *Eur. J. Oper. Res.*, vol. 175, pp. 1435–1446, 2006.

[5] N. Bekiaris-Liberis, C. Roncoli, and M. Papageorgiou, "Highway traffic estimation with mixed connected and conventional vehicles," in *Proc. IEEE CDC*, 2015, pp. 2806–2811. [Online]. Available: http://arxiv.org/abs/1504.06879

[6] A. Bose and P. Ioannou, "Mixed manual/semi-automated traffic: A macroscopic analysis," *Transp. Res. C, Emerging Technol.*, vol. 11, no. 6, pp. 439–462, Dec. 2003.

[7] A. Bose and P. Ioannou, "Analysis of traffic flow with mixed manual and semiautomated vehicles," *IEEE Trans. Intell. Transp. Syst.*, vol. 4, no. 4, pp. 173–188, Jan. 2004.

[8] L. C. Davis, "Effect of adaptive cruise control systems on mixed traffic flow near an on-ramp," *Physica A*, vol. 379, pp. 274–290, 2007.

[9] C. de Fabritiis, R. Ragona, and G. Valenti, "Traffic estimation and prediction based on real time floating car data," in *Proc. IEEE Conf. Intell. Transp. Syst.*, Beijing, China, 2008, pp. 197–203.

[10] W. Deng, H. Lei, and X. Zhou, "Traffic state estimation and uncertainty quantification based on heterogeneous data sources: A three detector approach," *Transp. Res. B, Methodol.*, vol. 57, pp. 132–157, Nov. 2013.

[11] C. Diakaki, M. Papageorgiou, I. Papamichail, and I. K. Nikolos, "Overview and analysis of vehicle automation and communication systems from a motorway traffic management perspective," *Transp. Res. A, Policy Pract.*, vol. 75, pp. 147–165, May 2015.

[12] J. I. Ge and G. Orosz, "Dynamics of connected vehicle systems with delayed acceleration feedback," *Transp. Res. C, Emerging Technol.*, vol. 46, pp. 46–64, Sep. 2014.

[13] J. C. Herrera and A. M. Bayen, "Incorporation of Lagrangian measurements in freeway traffic state estimation," *Transp. Res. B, Methodol.*, vol. 44, no. 4, pp. 460–481, May 2010.

[14] J. C. Herrera *et al.*, "Evaluation of traffic data obtained via GPS-enabled mobile phones: The Mobile Century field experiment," *Transp. Res. C, Emerging Technol.*, vol. 18, no. 4, pp. 568–583, Aug. 2010.

[15] A. Hegyi, D. Girimonte, R. Babuska, and B. De Schutter, "A comparison of filter configurations for freeway traffic state estimation," in *Proc. IEEE Conf. ITS*, Toronto, ON, Canada, 2006, pp. 1029–1034.

[16] A. Kesting, M. Treiber, M. Schonhof, and D. Helbing, "Adaptive cruise control design for active congestion avoidance," *Transp. Res. C, Emerging Technol.*, vol. 16, no. 6, pp. 668–683, Dec. 2008.

[17] S.-C. Lo and C.-H. Hsu, "Cellular automata simulation for mixed manual and automated control traffic," *Math. Comput. Modell.*, vol. 51, no. 7/8, pp. 1000–1007, Apr. 2010.

[18] E. Lovisari, C. Canudas de Wit, and A. Kibangou, "Flow and density reconstruction and optimal sensor placement for road transportation networks," *arXiv:1507.07093*, to be published.

[19] L. Mihaylova, R. Boel, and A. Hegyi, "Freeway traffic estimation within particle filtering framework," *Automatica*, vol. 43, pp. 290–300, 2007.

[20] M. Montanino and V. Punzo, "Making NGSIM data usable for studies on traffic flow theory," *Transp. Res. Rec.*, vol. 2390, pp. 99–111, 2013.

[21] M. Montanino and V. Punzo, "Reconstructed NGSIM I80-1," COST ACTION TU0903—MULTITUDE, 2013. [Online]. Available: www.multitude-project.eu/exchange/101.html

[22] I.-C. Morarescu and C. Canudas de Wit, "Highway traffic model-based density estimation," in *Proc. IEEE ACC*, San Francisco, CA, USA, 2011, pp. 2012–2017.

[23] J. B. Moore and B. D. O. Anderson, "Coping with singular transition matrices in estimation and control stability theory," *Int. J. Control*, vol. 31, no. 3, pp. 571–586, 1980.

[24] F. Morbidi, L.-L. Ojeda, C. Canudas de Wit, and I. Bellicot, "A new robust approach for highway traffic density estimation," in *Proc. IEEE ECC*, 2014, pp. 2575–2580.

[25] L. Munoz, X. Sun, R. Horowitz, and L. Alvarez, "Traffic density estimation with the cell transmission model," in *Proc. IEEE ACC*, 2003, pp. 3750–3755.

[26] D. Ngoduy, S. P. Hoogendoorn, and R. Liu, "Continuum modeling of cooperative traffic flow dynamics," *Phys. A, Statist. Mech. Appl.*, vol. 388, pp. 2705–2716, 2009.

[27] Q. Ou, R. L. Bertini, J. W. C. van Lint, and S. P. Hoogendoorn, "A theoretical framework for traffic speed estimation by fusing low-resolution probe vehicle data," *IEEE Trans. Intell. Transp. Syst.*, vol. 12, no. 3, pp. 747–756, Sep. 2011.

[28] M. Papageorgiou and A. Messmer, "METANET: A macroscopic simulation program for motorway networks," *Traffic Eng. Control*, vol. 31, no. 9, pp. 466–470, 1990.

[29] B. Piccoli, K. Han, T. L. Friesz, T. Yao, and J. Tang, "Second-order models and traffic data from mobile sensors," *Transp. Res. C, Emerging Technol.*, vol. 52, pp. 32–56, Mar. 2015.

[30] V. Punzo, M. T. Borzacchiello, and B. Ciuffo, "On the assessment of vehicle trajectory data accuracy and application to the Next Generation SIMulation (NGSIM) program data," *Transp. Res. C, Emerging Technol.*, vol. 19, no. 6, pp. 1243–1262, Dec. 2011.

[31] M. Rahmani, H. Koutsopoulos, and A. Ranganathan, "Requirements and potential of GPS-based floating car data for traffic management: Stockholm case study," in *Proc. IEEE Conf. ITS*, Funchal, Portugal, 2010, pp. 730–735.

[32] R. Rajamani and S. Shladover, "An experimental comparative study of autonomous and cooperative vehicle-follower control systems," *Transp. Res. C, Emerging Technol.*, vol. 9, no. 1, pp. 15–31, Feb. 2001.

[33] B. Rao and P. Varaiya, "Roadside intelligence for flow control in an intelligent vehicle and highway system," *Transp. Res. C, Emerging Technol.*, vol. 2, no. 1, pp. 49–72, Mar. 1994.

[34] C. Roncoli, M. Papageorgiou, and I. Papamichail, "Optimal control for multi-lane motorways in presence of vehicle automation and communication systems," in *Proc. IFAC World Congr.*, South Africa, 2014, pp. 4178–4183.

[35] C. Roncoli, I. Papamichail, and M. Papageorgiou, "Model predictive control for multi-lane motorways in presence of VACS," in *Proc. IEEE Conf. Intell. Transp. Syst.*, Qingdao, China, 2014, pp. 501–507.

[36] C. Roncoli, M. Papageorgiou, and I. Papamichail, "An optimisation-oriented first-order multi-lane model for motorway traffic," Transp. Res. Board, Washington, DC, USA, 2015.

[37] T. Seo, T. Kusakabe, and Y. Asakura, "Estimation of flow and density using probe vehicles with spacing measurement equipment," *Transp. Res. C*, vol. 53, pp. 134–150, Apr. 2015.

[38] S. E. Shladover, D. Su, and X.-Y. Lu, "Impacts of cooperative adaptive cruise control on freeway traffic flow," *Transp. Res. Rec.*, vol. 2324, pp. 63–70, 2012.

[39] M. Treiber, A. Kesting, and R. E. Wilson, "Reconstructing the traffic state by fusion of heterogeneous data," *Comput.-Aided Civil Infrastructure Eng.*, vol. 26, pp. 408–419, 2011.

[40] "Next Generation SIMulation (NGSIM)," U.S. Dept. Transp., Washington, DC, USA, 2005. [Online]. Available: www.ngsim-community.org

[41] B. van Arem, C. van Driel, and R. Visser, "The impact of cooperative adaptive cruise control on traffic-flow characteristics," *IEEE Trans. Intell. Transp. Syst.*, vol. 7, no. 4, pp. 429–436, Dec. 2006.

[42] J. W. C. van Lint and S. P. Hoogendoorn, "A robust and efficient method for fusing heterogeneous data from traffic sensors on freeways," *Comput.-Aided Civil Infrast. Eng.*, vol. 25, pp. 596–612, 2010.

[43] P. Varaiya, "Smart cars on smart roads: Problems of control," *IEEE Trans. Autom. Control*, vol. 38, no. 2, pp. 195–207, Feb. 1993.

[44] M. Wang, W. Daamen, S. P. Hoogendoorn, and B. van Arem, "Rolling horizon control framework for driver assistance systems. Part II: Cooperative sensing and cooperative control," *Transp. Res. C, Emerging Technol.*, vol. 40, pp. 290–311, Mar. 2014.

[45] Y. Wang and M. Papageorgiou, "Real-time freeway traffic state estimation based on extended Kalman filter: A general approach," *Transp. Res. B, Methodol.*, vol. 39, no. 2, pp. 141–167, Feb. 2005.

[46] Y. Wang *et al.*, "An adaptive freeway traffic state estimator," *Automatica*, vol. 45, no. 1, pp. 10–24, Jan. 2009.

[47] D. B. Work *et al.*, "An ensemble Kalman filtering approach to highway traffic estimation using GPS enabled mobile devices," in *Proc. IEEE CDC*, 2008, pp. 5062–5068.

[48] J. Yi and R. Horowitz, "Macroscopic traffic flow propagation stability for adaptive cruise controlled vehicles," *Transp. Res. C, Emerging Technol.*, vol. 14, no. 2, pp. 81–95, Apr. 2006.

[49] Y. Yuan, J. W. C. van Lint, R. E. Wilson, F. van Wageningen-Kessels, and S. P. Hoogendoorn, "Real-time Lagrangian traffic state estimator for freeways," *IEEE Trans. Intel. Transp. Syst.*, vol. 13, pp. 59–70, Mar. 2012.

[50] Y. Yuan, J. W. C. van Lint, R. E. Wilson, F. van Wageningen-Kessels, and S. P. Hoogendoorn, "Network-wide traffic state estimation using loop detector and floating car data," *J. Intel. Transp. Syst., Technol., Plan., Oper.*, vol. 18, pp. 41–50, 2014.

[51] L. Zhang and G. Orosz, "Stability analysis of nonlinear connected vehicle systems," in *Proc. ASME DSCC*, San Antonio, TX, USA, 2014, pp. 1–10.

Nikolaos Bekiaris-Liberis received the Ph.D. degree from the University of California, San Diego, CA, USA, in 2013.

From 2013 to 2014, he was a Postdoctoral Researcher with the University of California, Berkeley, CA. He is currently a Postdoctoral Researcher with the Dynamic Systems and Simulation Laboratory, Technical University of Crete, Chania, Greece. He has coauthored the Society for Industrial and Applied Mathematics book *Nonlinear Control under Nonconstant Delays*. His research interests include delay systems, distributed parameter systems, nonlinear control, and their applications.

Dr. Bekiaris-Liberis was a finalist for the Student Best Paper Award at the 2010 ASME Dynamic Systems and Control Conference and the 2013 IEEE Conference on Decision and Control. He received the Chancellor's Dissertation Medal in Engineering from the University of California, San Diego, in 2014.

Claudio Roncoli received the B.Sc. degree, the M.Sc. degree in computer science engineering, and the Ph.D. degree in system monitoring and environmental risk management from the University of Genova, Genova, Italy, in 2006, 2009, and 2013, respectively.

From 2007 to 2013, he was a Research Assistant with the Department of Communication Computer and System Sciences, Genova, working on the design and development of software in projects regarding transportation of dangerous goods, both within European research projects and with Eni, which is the most important Italian petrochemical company. During his Ph.D. studies, in 2011 and 2012, he was a Visiting Student with the Center for Transport Studies, Imperial College London, London, U.K. Since May 2013, he has been a Postdoctoral Research Associate with the Dynamic Systems and Simulation Laboratory, Technical University of Crete, Chania, Greece. His research interest is in automatic control, mainly applied to traffic and transportation management, traffic flow modeling, and computer-based decision support methodologies.

Markos Papageorgiou (F'99) received the Dipl.-Ing. and Dr.-Ing. degrees (honors) in electrical engineering from the Technical University of Munich, Munich, Germany, in 1976 and 1981, respectively.

He was a Free Associate with Dorsch Consult, Munich during 1982–1988 and with the Institute National de Recherche sur les Transports et leur Sécurité (INRETS), Arcueil, France, during 1986–1988. From 1988 to 1994, he was a Professor of automation with the Technical University of Munich. Since 1994, he has been a Professor with the Technical University of Crete, Chania, Greece. He was a Visiting Professor with the Politecnico di Milano, Milano, Italy, in 1982; with the École Nationale des Ponts et Chaussées, Paris, France, during 1985–1987; and with the Massachusetts Institute of Technology, Cambridge, MA, USA, in 1997 and 2000. He was also a Visiting Scholar with the University of California, Berkeley, CA, USA, in 1993, 1997, 2001, and 2011 and with other universities. He is an author or an editor of five books and of some 400 technical papers. His research interests include automatic control and optimization theory and applications to traffic and transportation systems, water systems, and further areas.

Dr. Papageorgiou was the Editor-in-Chief of *Transportation Research—Part C* (2005–2012). He also served as an Associate Editor for the IEEE Control Systems Society—Conference Editorial Board of the IEEE TRANSACTIONS ON INTELLIGENT TRANSPORTATION SYSTEMS and other journals. He is a Fellow of the International Federation of Automatic Control (2013). He received a German Academic Exchange Service (DAAD) Scholarship (1971–1976), the 1983 Eugen-Hartmann Award from the Union of German Engineers (VDI), and a Fulbright Lecturing/Research Award (1997). He was a recipient of the IEEE Intelligent Transportation Systems Society Outstanding Research Award (2007) and of the IEEE Control Systems Society Transition to Practice Award (2010). He was presented the title of Visiting Professor by the University of Belgrade, Belgrade, Serbia (2010). The Dynamic Systems and Simulation Laboratory he has been heading since 1994 received the IEEE Intelligent Transportation Systems Society ITS Institutional Lead Award (2011). He was also awarded a European Research Council Advanced Investigator Grant (2013–2017).